



Determination of Paris law constants with a reverse engineering technique

R. Branco^{a,*}, F.V. Antunes^b, J.A. Martins Ferreira^b, J.M. Silva^c

^a *Department of Mechanical Engineering, Polytechnic Institute of Coimbra, 3030-129 Coimbra, Portugal*

^b *Department of Mechanical Engineering, University of Coimbra, Pinhal de Marrocos, 3030-201 Coimbra, Portugal*

^c *Department of Aerospace Sciences, University of Beira Interior, 6200-001 Covilhã, Portugal*

Abstract

Paris law constants are commonly obtained with a well established procedure based on standard specimens, notched and pre-cracked. Pre-cracking produces through cracks with stable shapes, nearly straight, similar during all propagation. However, in several situations specimens with corner and surface cracks are recommended. In these cases cracks having significant propagation will continuously modify their shape, beginning with corner or surface geometries and subsequently transforming into through cracks, resulting into a transition region with significant crack shape modification. The aim of this paper is to determine Paris law constants from the analysis of crack shapes on the surface of fracture, in regions of intense shape modification. A double-U specimen of a new generation nickel base superalloy was used to obtain experimental crack shapes within transitory region as well as the number of load cycles between them. An automatic crack growth technique based on the finite element method (FEM) was employed to obtain fatigue constants from crack propagation data.

© 2008 Elsevier Ltd. All rights reserved.

Keywords: Paris law constants; Double-U specimen; Crack shape evolution; Reverse engineering

1. Introduction

Designers must be able to predict fatigue life in structures submitted to cyclic loads. Modern defect-tolerant design approaches to fatigue are based on the premise that engineering structures are inherently flawed, i.e., manufacturing defects are potentially present. The prediction of propagation life is usually based on Paris law:

$$\frac{da}{dN} = C\Delta K^m \quad (1)$$

being ΔK the range of stress intensity factor, and C , m constants that depend on material, stress ratio, temperature, etc. A well established procedure is used in order to determine the Paris law constants, considering

* Corresponding author. Tel.: +351 239 790 700; fax: +351 239 790 701.

E-mail address: rbranco@isec.pt (R. Branco).

standard specimens, notched and pre-cracked. BS 6835:1988 and ASTM 647-95a standards define all the details necessary to obtain feasible and comparable Paris law constants. However, the application of results from through-crack specimens referred in these standards to corner and surface cracks is not straightforward. Tong et al. [1] and Brown and Hicks [2] found that the use of results from CT specimens to corner cracks gave pessimistic life predictions, i.e., the fatigue life was underestimated. Therefore, taking into consideration that corner and surface cracks are quite frequent, alternative specimen geometries have been developed. A specimen with central hole and corner crack was used to study fatigue initiation and propagation in kitchen sinks [3]. The fatigue propagation in new generation nickel base superalloys, such as Udimet 720 or RR1000, has been studied using specimens representative of gas turbine discs in terms of notch geometry and bulk stress, such as the corner crack [4], the double-U or the washer specimens [5].

Numerical techniques have been successfully used to predict crack shape evolution and fatigue life. One of the most powerful and widely employed techniques described in literature consists of an iterative procedure based on a three-dimensional finite element analysis [6]. Firstly, a numerical model is developed to calculate the displacement field which is used to obtain the stress intensity factors along crack front. A new crack front position and the number of cycles are defined applying an adequate crack growth model, based on experimental $da/dN-\Delta K$ curves. This procedure is then repeated up to the final fracture when the fracture toughness is reached.

The aim of this paper is to propose an experimental–numerical technique oriented to the determination of Paris law constants from propagation regions with significant crack shape modification. Experimental work is required to obtain at least two crack shapes with significant shape modification and the number of load cycles between them. In this work, a double-U specimen of a new generation nickel base superalloy was tested experimentally. Original corner cracks transform into subsequent through cracks and a significant transition region was observed. Intentional marking of fracture surfaces was obtained either by changing stress ratio or loading frequency. An automatic crack growth technique based on the finite element method (FEM) was developed and employed to obtain Paris law constants from transient crack shapes. The Paris law constants C and m are obtained from crack shape change and from the number of load cycles, respectively.

2. Experimental determination of transient crack shapes

The geometry of the double-U specimen employed in this study is presented in Fig. 1. This specimen was developed to reproduce the geometry of a turbine disc at the region of its connection with the blades, since this is a high stress concentration zone prone to fatigue failures. The material considered in this investigation was the nickel base superalloy RR1000 developed by Rolls-Royce for specific usage in turbine discs and high pressure compressors of aeroengines. All tests were performed at 650 °C in a servo hydraulic testing machine with a 100 kN load capacity. Testing temperature was obtained via an electrical furnace. The mechanical properties and the chemical composition of RR1000 at room temperature and at 650 °C are presented in Tables 1 and 2, respectively. Fatigue tests were performed with a load ratio of 0.1 considering two waveforms: sinusoidal with a 5 Hz frequency and trapezoidal with a 30 s dwell time (1–30–1–1 s). A potential drop technique was used for crack propagation monitoring purposes using a DCPD pulsed system coupled with the controller of the servo hydraulic machine. During the tests the loading conditions (either stress ratio or loading frequency) were changed to produce visible marks on the fracture surface which enable the identification of crack shapes. Fig. 2a shows the fracture surface of a specimen submitted to a fatigue test using a sinusoidal load, while

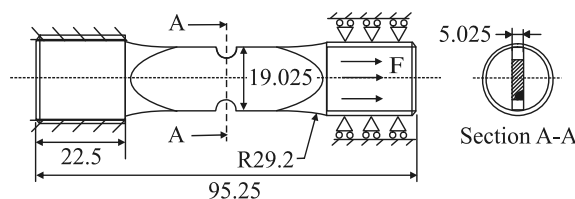


Fig. 1. Double-U specimen (dimensions in mm).

Table 1
Mechanical properties of RR1000 [5]

	Room temperature	650 °C
E (GPa)	214	188.6
0.2% Proof. (MPa)	1086	1034
UTS (MPa)	1602	1448
Poisson's ratio, ν		0.255

Table 2
Chemical composition of RR1000 (mass percentage)

Ni	Co	Cr	Mo	Ta	Ti	Al	B	C	Zr	Hf
52.4	18.5	15.0	5.0	2.0	3.6	3.0	0.015	0.027	0.06	0.07

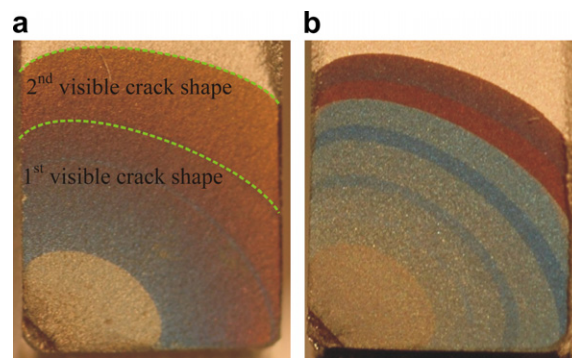


Fig. 2. Fracture surfaces (a) LF010 specimen: tested with a 5 Hz sinusoidal load, $R = 0.1$. (b) LF016 specimen: tested with a 1–30–1–1 s trapezoidal load, $R = 0.1$.

Fig. 2b presents the crack patterns for a different specimen tested with a trapezoidal load. First and second visible crack shapes of Fig. 2a were used to demonstrate the proposed procedure. As we can see crack shape changes as it propagates, having a typical elliptical geometry for the first stages of testing and a kind of modified through crack geometry near the end of testing.

3. Numerical procedure

The double-U specimen geometry employed in this investigation (see Fig. 1) has a 5.025 mm thickness and the radius of the semicircular notches is 2.379 mm. The screws at the extremities are used for fixing the specimen at the testing machine. Fig. 3a presents the physical model defined in this work. The specimen is sym-

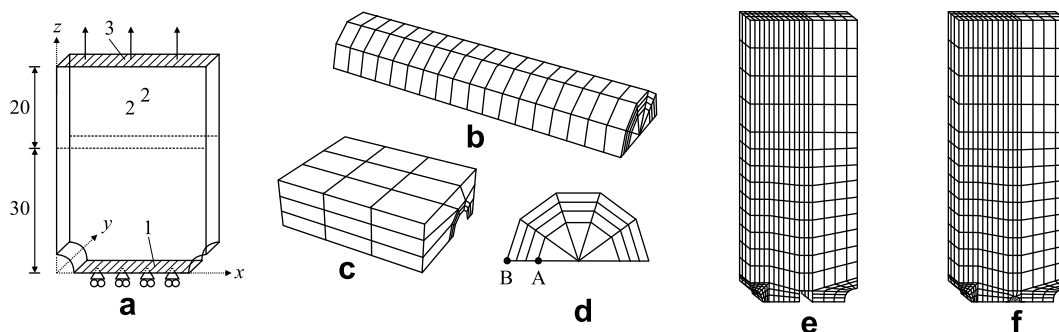


Fig. 3. (a) Physical model; (b) spider web mesh; (c) transition mesh; (d) spider web pattern; (e) regular mesh; and (f) assembled model.

metric in terms of geometry, loading and boundary conditions, therefore only half of it was considered for simulation purposes. Adequate boundary conditions are required to enforce the symmetry condition ($z = 0$ in region 1). The geometry of the extremities was simplified taking into consideration their remote position relatively to the crack front. A uniform load was applied at the extremity, as illustrated in Fig. 3a. The movement of the head (both regions 2) were restrained along x and y to simulate the constraint imposed by the high rigidity of the loading machine grips. The corner crack is plane, normal to the axis of the specimen and crosses its middle-section, leading to a mode-I loading along the whole crack front. The material was assumed to be continuous, homogeneous, isotropic and with linear elastic behaviour.

A 3D finite element model was developed and implemented using ModuleF, a non-commercial finite element package. The main difficulty of the finite element model is associated with the generation of finite element meshes for the cracked geometry. The crack front was divided into 18 elements, which correspond to 19 corner nodes (see Figs. 3b and 4). The mesh around each corner node has a spider web pattern consisting of four concentric rings (Fig. 3d) leading to the 3D spider web mesh shown in Fig. 3b. At remote positions from the crack front the mesh has a large regular pattern, with 3 elements along the thickness, in order to reduce the computational effort (Fig. 3e). The transition mesh (Fig. 3c) promotes the compatibility between both spider and regular meshes. The assembled model is presented in Fig. 3f. The model was defined parametrically, so physical variables, such as the thickness or notches' radius, can be easily modified. Isoparametric pentahedric singular elements (with mid-side nodes positioned at quarter point positions) were considered around the crack front. 3D isoparametric elements were considered elsewhere: 20-node hexahedral elements and 15-node pentahedric elements. A full Gauss integration was used, i.e., $3 \times 3 \times 3$ integration points for the hexahedric elements and 21 integration points for the pentahedric elements. The model contains 1837 nodes and 1359 elements (195 pentahedric elements and 1164 hexahedral elements). The mid-side nodes along the crack front were positioned on a cubic spline, which provides a good simulation of the real crack shape.

The stress intensity factors along the crack front (K) were calculated using a direct K calculation procedure. The extrapolation method with 2 points, uses the stress intensity factor values calculated at points A and B (see Fig. 3d), by:

$$K_1 = \sqrt{\frac{\pi}{8r}} \times \frac{E}{1 - \nu^2} \times v_p \quad (2)$$

where v_p is the crack opening displacement, r is the radial distance from crack tip, E and ν are the elastic constants assuming an isotropic behaviour. The pairs (r_A, K_{IA}) and (r_B, K_{IB}) are used to extrapolate the stress intensity factor to the crack tip ($r = 0$). The local K values and experimental Paris law constants are used to propagate the crack. The propagation at each crack front node, under remote mode-I loading, occurs along a direction normal to the crack front. The crack increment at an arbitrary node along the crack front was defined according to:

$$\Delta a_i^{(j)} = \left[\frac{\Delta K^{(j)}}{\Delta K_{\max}^{(j)}} \right]^m \Delta a_{\max}^{(j)} \quad (3)$$

where $\Delta a_{\max}^{(j)}$ is defined as a fraction of the average crack length for the j th iteration. Once ΔK varies with crack growth, Euler algorithm can be used to calculate the number of load cycles, leading to:

$$N^{(j+1)} = N^{(j)} + \Delta N^{(j)} \iff N^{(j+1)} = N^{(j)} + \frac{\Delta a_{\max}^{(j)}}{C[\Delta K_{\max}^{(j)}]^m} \quad (4)$$

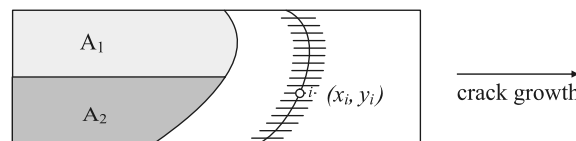


Fig. 4. Definition of the dependent parameter Z considered for the determination of the m constant.

Adding the crack increments defined by Eq. (3) to the actual nodal coordinates, a new crack front is created. Finally, some adjustments on the crack front are needed near the surface, in order to improve the quality of the mesh.

The procedure consisting of FEM analysis, K calculation and crack propagation can be repeated up to final fracture, which occurs when maximum stress intensity factor reaches the fracture toughness. Numerical errors must be minimized to obtain feasible predictions; therefore the parameters affecting the accuracy must be identified and optimized. A detailed identification and optimization of these parameters can be found elsewhere [7,8].

4. Presentation and analysis of results

The application of the proposed methodology requires a robust parameterization of crack shape and crack length. Two main groups of parameters can be distinguished: global parameters which quantify the shape of all crack and local parameters which study the behaviour of few specific nodes [7,8]. Herein, it was used a global parameter (Z) given by the ratio A_1/A_2 , where A_1 and A_2 are, respectively, the light and dark areas shown in Fig. 4 (the half thickness divides both zones). During the propagation, this parameter tends to unity once the crack follows towards a symmetrical shape. This parameter is adequate to characterize asymmetrical crack shapes as well as to observe the asymmetrical degree during the propagation. Besides, this parameter presents a high sensitivity to the exponent of Paris law (m) which is very useful for its determination. The sensitivity of Z to the exponent of Paris law will be clearly presented afterwards. The C constant of Paris law has a great influence on fatigue life, therefore the number of load cycles (N) between two well defined crack shapes was used to calculate C .

The calculation of both Paris law constants can be started after the selection of dependent parameters. The first crack shape was divided into 19 layers (see Fig. 4), corresponding to the layers of the spider web mesh. Both x_i and y_i coordinates were measured, being the former the crack length and the latter the position along the thickness for the i th-division. These coordinates were directly used to define the initial crack on the FEM model. All numerical variables were fixed taking into consideration previous optimization studies [7,8]. A set of independent numerical propagations was carried out, with values of m between 1 and 5, with constant increments of 0.25. Fig. 5a presents the evolution of Z with average crack length (\bar{a}) for different values of m . In this case, abscises consist of a modified average crack length (a), which was obtained subtracting the initial average crack length to the actual average crack length. In other words, the modified average crack length is forced to start from 0.

The curves in Fig. 5a tend towards unity, i.e., tend to achieve symmetrical crack shapes. This was expected considering the symmetry of specimen in terms of geometry, loading and material. As the exponent of Paris law rises, a faster convergence of Z towards the unity is observed. This was expected considering that higher

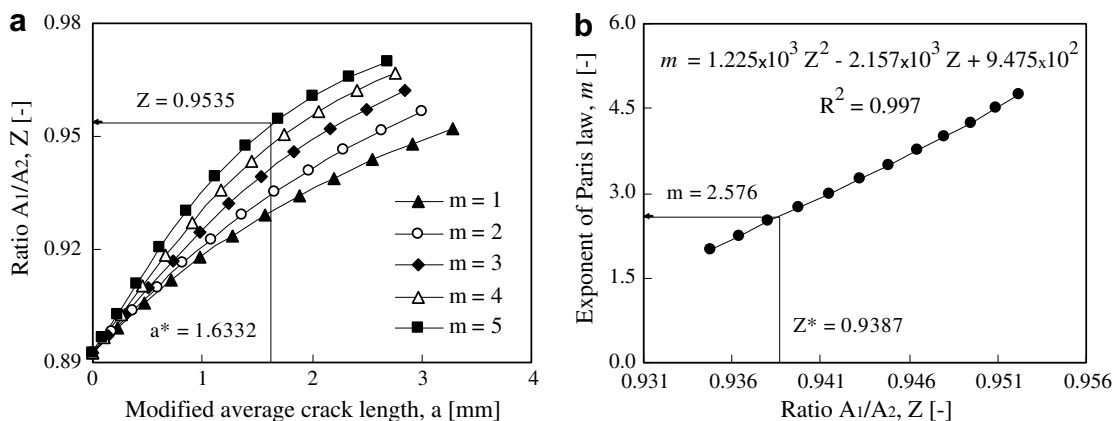


Fig. 5. Determination of m constant of Paris law: (a) evolution of the ratio A_1/A_2 with the modified average crack length; (b) evolution of m with the ratio of A_1/A_2 .

values of m are always responsible for faster crack shape modifications. The ratio A_1/A_2 has a high sensitivity to m , i.e., a significantly different trajectory is followed by the crack for each value of the exponent of Paris law, which can be taken as an evidence of the robustness of Z and its suitability to find the m constant.

Next step was the analysis of first and second visible crack shapes, on the fracture surface of Fig. 2a. The average crack lengths and the sets of x_i and y_i coordinates were calculated for each one. Subtraction of the initial average crack length (average crack length of the first visible crack shape) from the final average crack length gives the experimental modified average crack length (a^*). The number of fatigue cycles between both visible crack shapes (N^*) and the experimental ratio A_1/A_2 for second visible crack shape (Z^*) were obtained. In the present study, these experimental values (a^* , N^* and Z^*) were, respectively, 1.6323 mm, 5640 cycles and 0.9387. The value of a^* was used to define a function relating the ratio A_1/A_2 with the exponent of Paris law. For each value of m an unequivocal value of Z can be calculated (as schematically presented in Fig. 5a for m equal to 5). Repetition of this procedure for the remaining curves gives the results in Fig. 5b, which can be fitted by a second-order polynomial function, as follows:

$$m(Z) = 1225 \times 10^3 Z^2 - 2157 \times 10^3 Z + 9475 \times 10^2 \quad (5)$$

Finally, by substituting the value of Z^* in the function found previously we are able to find the m constant for the present case. Thus, $m(Z = Z^*) = 2.567$, according to Fig. 5b.

A similar procedure was carried out in order to obtain the C constant of Paris law. In this case, the fatigue life was used as a dependent parameter. A set of numerical propagations taking into account different C constants was done. These values were chosen within the interval 1×10^{-6} to 5×10^{-8} with a constant increment of 5×10^{-8} . Fig. 6a shows the results obtained for the several cases. As well known, fatigue life raises when C constant decreases, which is clearly observed in this figure. Taking into account the value of a^* , a unique value of N can be selected for each C constant, as schematized in Fig. 5 for $C = 1 \times 10^{-7}$. Using these points it is possible to obtain a function which relates fatigue life with the C constant. A potential function is able to fit these variables adequately leading to the Eq. (6). As presented in Fig. 6b a square correlation about 0.999 was accounted.

$$C(N) = 5536 \times 10^{-4} N^{-0.995} \quad (6)$$

Finally, introducing the value of N^* in previous function, it is possible to find the correct value of the C for the present case. So, $C(N = N^*) = 9.479 \times 10^{-8}$, as presented in Fig. 6b.

4.1. Sensitivity analysis

A sensitivity analysis was developed in order to study the robustness of the values obtained for C and m . For m constant, for example, non-dimensional sensitivity is defined as

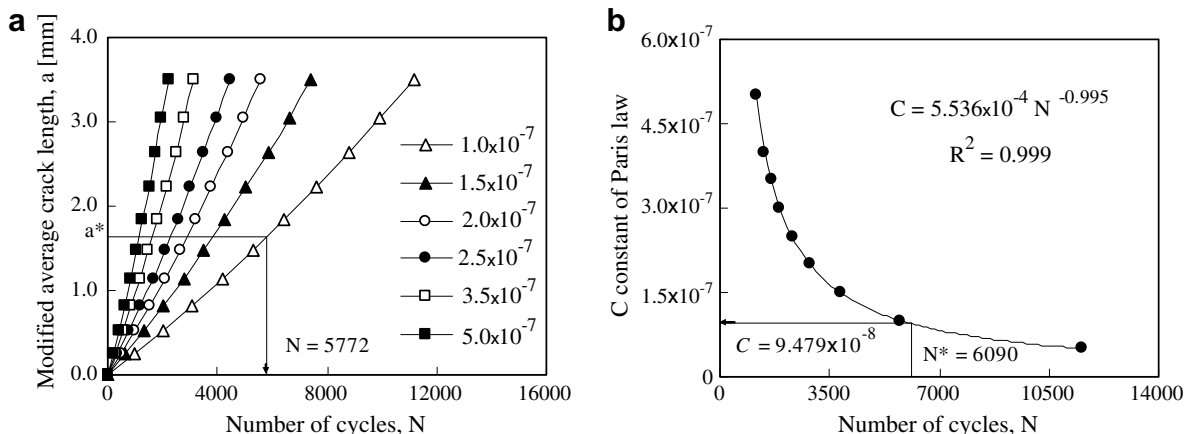


Fig. 6. Determination of c constant of Paris law: (a) evolution of the modified average crack length with the number of cycles; (b) evolution of C with the number of cycles.

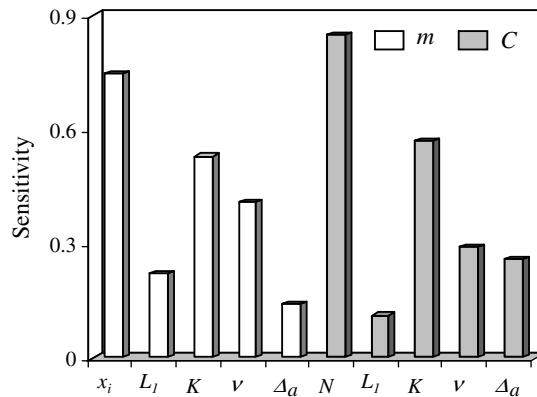


Fig. 7. Sensitivity analysis of the main independent parameters.

$$\nabla m = \frac{\partial m}{\partial p} \cdot \frac{p}{m} \quad (7)$$

being p a generic independent parameter. Notice that a sensitivity of 0.5 indicates that a variation of 1% in p produces a variation of 0.5% in m . Classical forward finite difference approach was used [9]:

$$\frac{\partial p}{\partial m} \approx \frac{m(p + \Delta p) - m(p)}{\Delta p} \quad (8)$$

Both final results C and m can be affected by a wide range of experimental and numerical variables. The former are associated with the input data. Accurate values of specimen's size, crack dimension, number of load cycles, mechanical properties and superficial phenomena are fundamental to develop an appropriated and representative numerical model. The latter are ascribed to the numerical procedure. Options, such as mesh topology, density of the layers of the mesh, type and size of crack front elements, crack front definition, K calculation method, crack increment, crack direction or fracture criterion cannot be ignored.

An exhaustive analysis of both types of variables lies beyond the scope of our present study and it would be extensive. Thus, critical variables were identified considering author's experience [7,8]: x_i and y_i coordinates, Poisson's ratio and number of fatigue cycles. In relation to the numerical parameters, following similar criterion, the most important are: radial size of crack front elements L_1 , K values and the crack increment Δa .

Perturbations (Δp) equal to $\pm 1\%$ were employed for each one of the variables mentioned earlier and the non-dimensional sensitivities were calculated for both C and m constants, except for x_i and N which were only calculated for m or C , respectively. The results are presented in Fig. 7. In relation to the m constant, the greatest sensitivity was found for x_i and y_i coordinates, which means that the crack shapes must be accurately measured on the fracture surfaces. Furthermore, concerning to the C constant, it is also observed a high impact in N , being its sensitivity the greatest in this case.

The other physical parameters have a lower influence but not negligible. K values have also a great impact in the final results which was also expected. Comparing sensitivities accounted for m and C , it is possible to conclude that, the latter are greater than the former, except for L_1 being inverted this behaviour. Besides, homologous sensitivities have similar magnitudes. It seems that the numerical procedure can be very stable once a high accuracy of x_i coordinates, K values and N is guaranteed.

5. Conclusions

The main conclusions of the present study are:

- An innovative reverse engineering technique based on the analysis of the surfaces of fracture and on automatic crack growth modelling was developed in order to obtain the Paris law constants (C , m). The technique is adequate to study regions with crack shape change, therefore extending the usage of specimens with corner and surface crack shapes.

- The technique was applied to a double-U specimen of RR100, a nickel base superalloy. Experimental work was developed to obtain crack shapes and fatigue life. A 3D finite element model was created to predict crack shape evolution. Values of $C = 9.479 \times 10^{-8}$; $m = 2.53$ were obtained for $R = 0.1$ and a loading frequency of 5 Hz.
- A sensitive analysis on the main numerical variables affecting the procedure was carried out. According to the results presented the procedure shows a significant sensitivity in relation to the physical and the numerical parameters earlier enunciated. Therefore all efforts are required to measure accurately the crack shapes, the number of cycles, Poisson's ratio and to obtain accurate values of K .

Acknowledgments

The authors acknowledge the financial support from Project POCTI-EME/46195/2002, promoted by Fundação para a Ciência e Tecnologia, Portugal.

References

- [1] Tong J, Byrne J, Hall R, Aliabadi MHA. Comparison of corner notched and compact tension specimens for high temperature fatigue testing. In: Proceedings of the conference engineering against fatigue, 17–21 March, University of Sheffield, UK.
- [2] Brown CW, Hicks HA. Fatigue growth of surface cracks in nickel-base superalloys. *Int J Fatigue* 1984;4:73–81.
- [3] Antunes FV, Martins Ferreira JA, Costa JD, Capela C. Fatigue life predictions in polymer particle composites. *Int J Fatigue* 2002;24:1095–105.
- [4] Antunes FV, Martins Ferreira JA, Branco CM, Byrne J. Influence of stress state on high temperature fatigue crack growth in Inconel 718. *Fatigue Fract Eng Mater Struct* 2001;24:127–35.
- [5] Cláudio R. Fatigue behaviour and structural integrity of scratch damaged shot peened surfaces at elevated temperature, PhD Thesis, University of Portsmouth, UK, December 2005.
- [6] Lin XB, Smith RA. Finite element modelling of fatigue crack growth of surface cracked plates. Part I: the numerical technique. *Eng Fract Mech* 1999;63:503–22.
- [7] Branco R, Antunes FV. Finite element modelling and analysis of crack shape evolution in mode-I fatigue middle-cracked tension specimens. *Eng Fract Mech* 2008;75(10):3020–37. doi:10.1016/j.engfracmech.2007.12.012.
- [8] Branco R. Numerical study of fatigue crack growth in MT specimens. MSc Thesis, Department of Mechanical Engineering, University of Coimbra, 2006 [in Portuguese].
- [9] Hafka H, Adelman H. Recent developments in structural sensitivity analysis. *Struct Optimizat* 1989;1:137–51.